Journal of Catalysis 286 (2012) 193–205

Contents lists available at SciVerse ScienceDirect

Journal of Catalysis

journal homepage: www.elsevier.com/locate/jcat

Sol–gel immobilization of octaethylporphine and hematoporphyrin for biomimetic photooxidation of α-pinene

Mariusz Trytek [a,*], Marek Majdan [b], Agnieszka Lipke [b], Jan Fiedurek [a]

[a] Department of Industrial Microbiology, Institute of Microbiology and Biotechnology, Maria Curie-Skłodowska University, 20-033 Lublin, Poland
[b] Faculty of Chemistry, Maria Curie-Skłodowska University, M. Curie-Skłodowskiej Sq. 2, 20-031 Lublin, Poland

ARTICLE INFO

Article history:
Received 9 September 2011
Revised 3 November 2011
Accepted 4 November 2011
Available online 15 December 2011

Keywords:
Sol–gel
Biomimetics
Photocatalysis
Porphyrins
Pinene
Fluorescent materials

ABSTRACT

The nature and aggregation of octaethylporphine (OEP) and hematoporphyrin (HmP–IX) immobilized in silica during the sol–gel process were evaluated using UV–Vis absorption, excitation and emission spectroscopies. An essential difference in biomimetic photooxidation of α-pinene was observed between the two obtained intensive luminescent materials. Biocatalytic activity was only found for OEP/SiO_2, and the lack of such activity for HmP–IX/SiO_2 was related to the interaction of its carboxyl groups with the silica structure. Myrtenol was the only primary and pinocarvone and pinocarveol the only secondary products of the reaction of α-pinene oxidation. A cooperative mechanism of photooxidation based on proton transfer between protonated porphyrin and silanol/siloxane groups followed by electron abstraction from substrate by the light-excited OEP/SiO_2 matrix or photosensitized generation of singlet oxygen ($^1O_2$) was proposed. The correlation between the biocatalytic efficiency and spectral properties of the porphyrins was also examined. The reusability and stability of OEP/SiO_2 were demonstrated in four catalytic cycles.

1. Introduction

Introduction of oxygen into olefinic terpene skeletons of α-pinene or *R*-(+)-limonene is an important reaction in the formation of a wide variety of different terpenoid derivatives found in the plant kingdom [1]. A number of oxygenated monoterpenes present at low concentrations in plant oils have flavoring/fragrance and anti-carcinogenic properties. It is not surprising then that significant efforts have been directed toward exploring these remarkable compounds and their alternative, synthetic sources.

Most of the microbial oxidations of terpenes described so far have been initiated by cytochrome-P450-dependent monooxygenases, i.e., heme-containing proteins responsible for catalytic insertion of oxygen into a large variety of substrates in a specific and regioselective way [1,2]. Porphyrins, especially metalloporphyrins in homogenous systems, due to their synthetic versatility and reactivity, are especially attractive for the construction of biomimetic analogs of oxygenases through elaboration of the superstructure of macrocycle or chelate complexes [3–9]. They also make it possible to carry out oxidation reactions in non-aqueous media, e.g., for C—H activation in monoterpene molecules under mild conditions. However, there are some important limitations to the application of metalloporphyrins, such as instability due to oxidative degradation of the porphyrin ring and difficulty of recovering these expensive compounds.

The use of heterogeneous catalysts offers advantages (such as easier recovery and recycling and increased stability) over those used in homogenous conditions. Therefore, many attempts have been made to incorporate porphyrin on solid supports, including the use of cross-linked polymers [10–14], clays and layered materials [15,16], biopolymers [17], polymeric ion-exchanging resins [18,19], silanized kaolinite [20], different types of zeolites [21,22] and modified silica [9].

At present, sol–gel processes offer new and promising possibilities for the direct bioencapsulation of porphyrin photocatalysts, as well as other active biological substances with heat-sensitive and fragile molecules, such as enzymes, proteins, antibodies and microbial whole cells. Besides simplicity of preparation, low-temperature encapsulation and tunable porosity, silica sol–gels are also characterized by optical transparency, chemical and photochemical inertness and photochemical, thermal and mechanical stability [23].

There are several reports on porphyrins immobilized in the sol–gel matrix as new functional catalytic devices for the production of commercially important compounds. For example, iron porphyrin catalysts have been anchored on spherical silica gel beads obtained by the sol–gel route for the oxidation of (*Z*)-cyclooctene and cyclohexane with PhIO or H_2O_2 [24–26]. In turn, silica microspheres functionalized with 5-(4-allyloxy)phenyl-10,15,20-tri(2,6-dichlorophenyl)porphyrin have been prepared by Huang et al. for the photooxidation of 1,5-dihydroxynaphthalene under visible light irradiation in an aerated aqueous solution [27]. Recently, a visible

* Corresponding author. Address: Department of Industrial Microbiology, Institute of Microbiology and Biotechnology, Maria Curie-Skłodowska University, Akademicka St. 19, 20-033 Lublin, Poland. Fax: +48 81 537 5959.
E-mail address: mtrytek1@o2.pl (M. Trytek).

0021-9517/$ - see front matter © 2011 Elsevier Inc. All rights reserved.
doi:10.1016/j.jcat.2011.11.005

light photocatalytic system based on water-insoluble tin porphyrin $Sn(OH)_2$(TPP) immobilized on SiO_2 has been successfully used for the degradation of 4-chlorophenol and acid orange 7 [28].

Pinenes are constituents of the wood and oil of an extensive variety of plants. One rich source of α-pinene is turpentine, a by-product of the pulping process in paper making. If an efficient method could be developed for conversion of non-polar turpentine monoterpenes into valuable flavor and fragrance compounds, the value of the product would be increased. It is worth mentioning that the method of oxidation of natural pinene by porphyrin immobilized on silica is a response to the global tendency for developing cleaner processes, according to the 3R rule (Reduce, Reuse, and Recycle).

A previous study has demonstrated that some porphyrins encapsulated in silica gel act as intensive luminescent materials and efficient catalysts in biomimetic photocatalytic systems [29]. Unfortunately, that study has made no reference to the influence of immobilization on the mechanism of photocatalysis. In this connection, the aim of the present work was to elucidate how the change of the physicochemical properties of porphyrins in sol–gel determines the efficiency and the mechanism of photocatalysis. An investigation of the differences in biomimetic oxidation of α-pinene by free-base, water-insoluble octaethylporphine (OEP) and hematoporphyrin (HmP–IX) intercalated in transparent sol–gel silica is also reported.

2. Materials and methods

2.1. Preparation of transparent monolithic gel-bars

Silica gels were prepared by sol–gel polymerization of tetraethylorthosilicate (TEOS). TEOS was polymerized by hydrolysis and condensation, with hydrogen chloride used as a hydrolysis catalyst. In a typical preparation of monoliths, 78 cm^3 of TEOS and 42 cm^3 of acidic water (HCl, pH approx. 3) were stirred for 1.5 h. The molar ratio of (HCl + H_2O) to TEOS was fixed at 6.7. After hydrolysis, a homogeneous sol was obtained, with a final pH of about 4.5. Next, 4-cm^3 portions of the sol were placed in disposable polystyrene spectrofluorimetric cells. Appropriate amounts of mother solutions of porphyrins in THF, at 10^{-3} M for HmP–IX and 5×10^{-4} M for OEP, were added (using Hamilton microsyringes) to the sol in the disposable spectrofluorimetric cells. Two parallel series of doped sols were prepared in which the concentrations of the porphyrins varied from 1×10^{-6} to 2.2×10^{-5} M. The final concentration in each series was dependent on the solubility of the particular porphyrin. Finally, the plastic cells were sealed with parafilm. Gelation was observed after 5 days. The material obtained at this stage was designated alcogel. After 1 month, the parafilm was perforated with a needle to allow slow evaporation of the solvent during monolith drying. The alcogels synthesized according to the above procedure had a structure filled with EtOH and water. Wet gels were dried at 23 °C in air.

The parafilm was removed after 5 months, and the drying process was continued until the volumes of the shrinking monoliths were constant and equal to approximately 1/8 of the volume of the alcogel samples, resulting in the formation of a material hereafter referred to as xerogel. Such a complicated procedure of slow drying was used to prevent cracking of the monolithic transparent gels.

2.2. Evaluation of textural properties of silica gel samples

The specific surface areas of the dried silica gel samples were calculated using the BET method [30], and their pore volumes were determined from low-temperature nitrogen adsorption measured using a Micrometrics ASAP 2405 V1.01 analyzer. Before measurements, the samples were degassed at −170 °C.

2.3. Spectral measurements

Absorption UV–Vis spectra of the porphyrins in solutions and gels were registered with a Carl-Zeis Jena M42 spectrophotometer in the 350–700 nm range at 23 °C, while emission spectra were recorded using an FP-6300 spectrofluorometer (JASCO). The UV–Vis spectra of solutions were registered in a 1 cm quartz cell, while the gel spectra were measured after the solid samples were withdrawn from the disposable cells. The fluorescence spectra were taken without filters, since the FP-6300 spectrofluorometer had sufficiently high resolutions, and the xenon lamp peaks did not interfere with the investigated spectra. The UV–Vis reflectance spectra were registered using a Horizontal Sampling Integrating Sphere (Model: PIV-756) connected to a V-660 Spectrophotometer (JASCO).

It should be noted that the structure and properties of doped sol–gels depend not only on the chemical composition of the starting materials, but also on numerous operational factors involved in the preparation of sol–gels such as the water/silica molar ratio, the type of solvent and catalyst, pH, temperature and humidity. These parameters highly influence hydrolysis and condensation. To eliminate these variations, all samples were prepared at the same time from one stock solution, and all spectra were performed on the same day. In this way, all assay reactions in one series of experiments were carried out in the same conditions.

2.4. Photooxidation experiments

As a final step, the dry samples, defined as xerogel, were firstly broken and then powdered in a mill (Planetary mill PULVERISETTE 6, Fritsch) to an average particle size of 0.2 mm for use in further experiments.

Photooxidation experiments were carried out under controlled temperature (20 °C), using an incubator consisting of four fluorescent visible lamps (Osram Lumilux, Cool White) arranged regularly above the reaction vessel. Catalytic oxidation was carried out at atmospheric pressure, under oxygen dissolved in the system in a closed 10-ml glass container equipped with a magnetic stirring bar. In a typical run, 150 μmol of α-pinene (corresponding to 50 mM) was dissolved in 3 cm^3 of chloroform (acetone or 1,4-dioxane) containing a predetermined amount of immobilized porphyrin in a powder form (200 mg) and irradiated under an estimated light intensity ranging from 120 to 150 μmol/m^2 s. Unless stated otherwise, the phototransformation of α-pinene was carried out for 24 h. In photodynamic experiments, the photoreactivity runs were carried out for 33 h. 50-μL samples were withdrawn from the suspensions every 1 h during the first 4 h of irradiation and subsequently every 4 or 12 h.

Silica powder was evenly dispersed in the organic solvent containing analytes during magnetic stirring. At the end of the appropriate time intervals, aliquots of 100 μl of the reaction medium were withdrawn and vigorously mixed with an equal volume of an internal standard solution of 0.05% (v/v) *n*-decane (for the substrate) and linalool (for the oxidation products) in hexane, to be subsequently used for GC and GC–MS analyses.

Since it is known that photooxygenation of pinene yields hydroperoxides [31], the resulting mixtures were treated with a 5% excess of the reducing agent triphenyl phosphine at room temperature for 2 h, to convert hydroperoxides to alcohols. The samples were analyzed by GC–MS.

2.5. Comparison of porphyrin photoactivity in a homogenous and a heterogeneous system

The substrate (150 μmol) in 3 mL of chloroform was mixed with an appropriate amount of photosensitizer (1.7×10^{-9} mol of

free-base OEP or 4.5×10^{-9} mol of free-base HmP–IX or an equivalent molar amount in 185 mg of encapsulated porphyrins in a powder form) to produce 1/117,647 and 1/44,444 M ratios of sensitizer (OEP or HmP–IX) to substrate, respectively. For both HmP–IX and OEP, two parallel experiments were performed for 24 h at 20 °C under the estimated intensity of visible light.

The stability and re-usability of the porphyrins were monitored using multiple sequential oxidation of pinene under conditions described above. Prior to each reaction cycle, the catalyst was filtered off, washed exhaustively with chloroform and methanol and dried on a rotary vacuum evaporator in a water bath at 50 °C. The procedure was repeated three times to remove any terpene residues. Finally, UV–Vis reflectance spectra of the catalyst were recorded before its retesting with a new reactant mixture.

2.6. Chromatographic analysis

Progress of the reaction (in terms of selectivity and conversion) was monitored using a Varian GC system fitted with a DB-5 capillary column and FID (Flame Ionization Detector). The reaction products were analyzed using a Phinigan DSQ spectrometer coupled to a Trace GC Ultra Chromatograph equipped with an RTX-5 column according to the method given in Ref. [29].

Compounds were identified by comparing their mass spectra and retention indexes (RI) with those of authentic sample spectra in a standard library database system. The volatile compounds were quantified by calculating the corresponding GC peak areas with respect to the GC peak area of the internal standard. Biotransformations were performed in two replicate samples, and analyses were carried out in duplicate. The errors associated with the GC quantification of samples were 5% and are quoted for a confidence interval of 95%. The presented data are reported as average values.

Hydroperoxides were identified by GC–MS using the split-injection/temperature-programmed sample introduction technique (PTV) and estimated on the basis of corresponding alcohols. Pinocarveyl hydroperoxide was the only hydroperoxide identified. Its mass spectra were as follows; [*m*/*z* (% of base peak)] 168 [M^+ (<0.2)], 153 [M^+-CH_3 (94)], 150 [M^+-H_2O (<0.1)], 109 (4), 97 (24), 83 (9), 71 (3), 70(100), 69 (8), 55 (22), 42 (9), 41 (31). Hydroperoxide yields were determined by double injection, with and without reduction of the reaction mixture by triphenylphosphine, and then calculated from the increase in alcohol content. The mass balance between pinocarvone and hydroperoxide, monitored by an internal standard, was above 90% in all cases. A detailed GC and MS analysis confirmed that pinocarveol represented a <90% yield based on hydroperoxide.

3. Results and discussion

3.1. Spectral behavior of porphyrins intercalated in silica gel

Physicochemical characterization of an active element is of primary importance at the initial stages of the design of a new photocatalytic device. The absorption and emission spectra of porphyrins are extremely sensitive to processes such as metalation, protonation, ring oxidation and dimerization. In all porphyrin spectra, two main bands can be distinguished in the region of 400–450 nm and 500–650 nm, which are known as the Soret and the Q bands, corresponding to electronic transitions of $S_0 \rightarrow S_2$ and $S_0 \rightarrow S_1$, respectively. The Soret band originates from allowed electronic transitions and is about 15–30 times more intensive than the Q band, which occurs as a result of forbidden electronic transitions.

The spectra of hematoporphyrin (HmP–IX) and octaethylporphine (OEP) in silica sol and alcogel (Figs. 1 and 2) were compared. In contrast to OEP, increasing concentrations of HmP–IX resulted in an evident straight-line increase in absorbance at 391 and 393 nm. The increase was probably caused by the strong solvation of the hydroxyl and carboxyl groups of HmP–IX by ethanol molecules. We did not observe any deviation from Beer's Law, which is evidence for the lack of aggregation of this porphyrin in the sol and alcogel matrix.

It has been reported that porphyrin molecules tend to aggregate by hydrophobic and π–π interactions, leading to a loss of linearity in the Beer's law plot [32]. Thus, a drastic decrease in Soret band intensity, which is the basis for the evaluation of the molar fractions of monomers, dimers and trimers of porphyrin, was observed with increasing concentrations of OEP. The following equations were used to estimate the dimerization and trimerization constants of OEP in sol–gel and the molar fractions of the particular species:

$$\varepsilon = \varepsilon_{mon}\alpha_{mon} + \varepsilon_{dim}\alpha_{dim} + \varepsilon_{trim}\alpha_{trim}, \quad (1)$$

where ε refers to molar absorbance, i.e., the A/c ratio (A – absorbance, c – molar concentration of porphyrin), and ε_{mon}, ε_{dim}, ε_{trim} denote molar absorbances of monomers, dimers and trimers of OEP (in L/mol×cm^{-1}). The symbol α refers to the molar fractions of the particular forms of porphyrin calculated from:

$$\alpha_{mon} = [OEP]/([OEP] + \beta_{dim}[OEP]^2 + \beta_{trim}[OEP]^3), \quad (2)$$

$$\alpha_{dim} = \beta_{dim}[OEP]^2/([OEP] + \beta_{dim}[OEP]^2 + \beta_{trim}[OEP]^3), \quad (3)$$

$$\alpha_{trim} = \beta_{trim}[OEP]^3/([OEP] + \beta_{dim}[OEP]^2 + \beta_{trim}[OEP]^3), \quad (4)$$

where [OEP] is the molar concentration of the OEP monomer, whereas β_{dim} and β_{trim} are dimerization and trimerization constants evaluated from the formulas:

$$\beta_{dim} = [(OEP)_2]/[OEP]^2, \quad (5)$$

$$\beta_{trim} = [(OEP)_3]/[OEP]^3. \quad (6)$$

$[(OEP)_2]$ and $[(OEP)_3]$ refer to the concentrations of dimers and trimers of OEP. The total concentration c of porphyrin has to fulfill the equation:

$$c = [OEP] + 2[(OEP)_2] + 3[(OEP)_3]. \quad (7)$$

There was a relatively good fit between the experimental ε values and those calculated from Eq. (1) as well as between the total porphyrin concentration c and that found from Eq. (7), namely $R^2 > 0.99$ (where R^2 is the determination coefficient). The fitting procedure was performed using PSI-PLOT (Version 8.83, Poly Software International). An evident increase in the molar fractions of dimers and a decrease in the molar fractions of trimers are observable when the sol sample is compared with the alcogel samples (Fig. 3). It seems that in sol, porphyrin molecules can freely form both dimers and trimers, whereas in the SiO_2 matrix, the formation of trimers and higher agglomerates is strongly limited due to geometrical constrains, namely the small pore dimensions that hinder the incorporation of the trimers into the gel skeleton. It is interesting to note that the molar absorbance coefficient for monomers ε_{mon} is in the range 10^5–10^6 L/mol×cm^{-1}, whereas the values of ε_{dim} and ε_{trim} are at the zero level, which was determined from the goodness of fit to Eqs. (1) and (7). This is probably the result of a π–π interaction between OEP molecules during the formation of dimers and trimers. Electrons participating in the π–π bond cannot be promoted to higher electronic states as easily as in the case of OEP monomers. Dimers and trimers of porphyrin in alcogel do not absorb light, but they alter the concentration of monomers, which is observable as a decrease in the absorbance with the rise in OEP concentration.

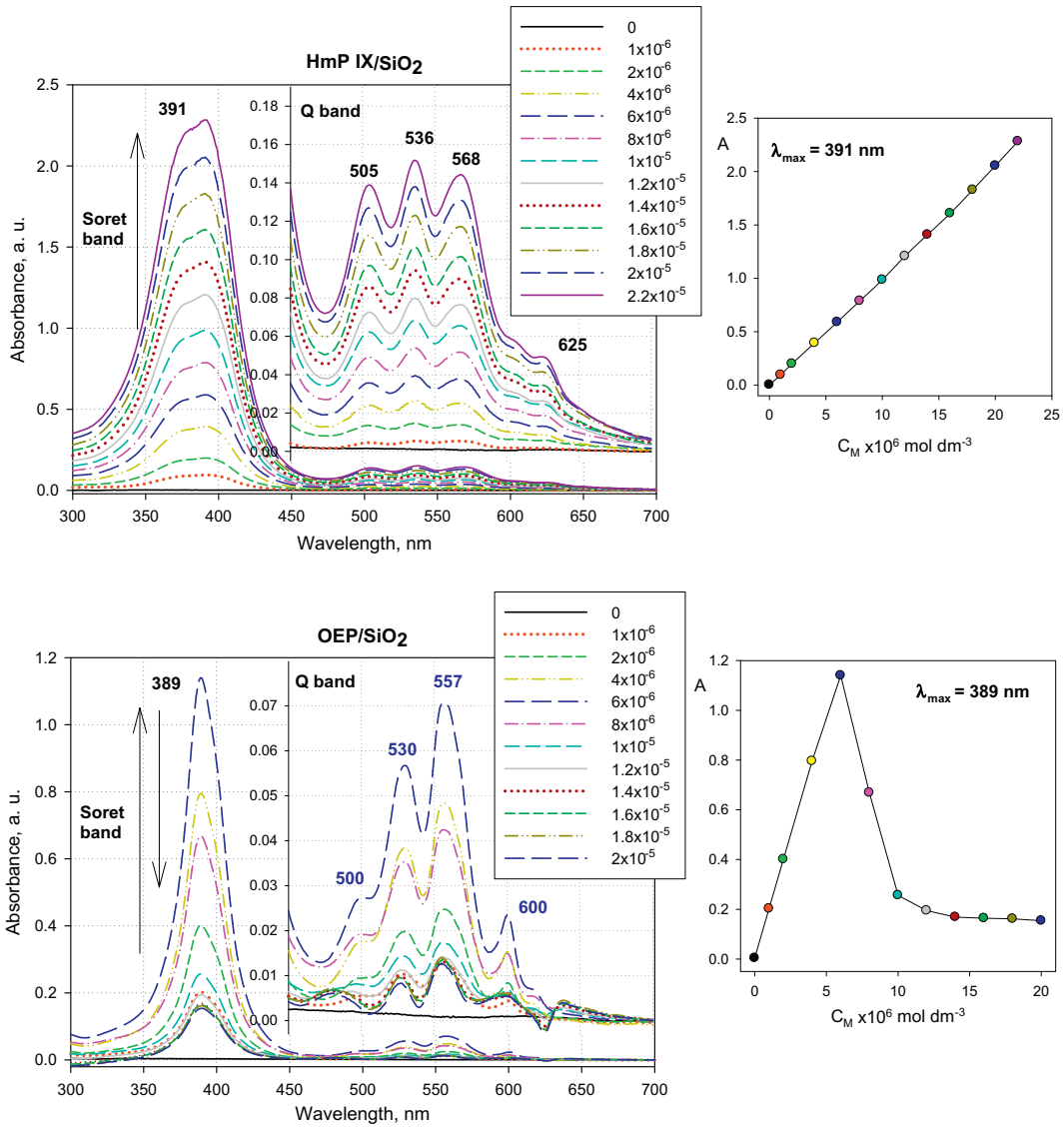

Fig. 1. UV–Vis absorption spectra of HmP–IX and OEP intercalated in SiO_2 sol (the numbers denote the concentrations of the porphyrins).

In xerogel, both OEP and HmP–IX behave similarly with regard to the character of their UV–Vis absorption spectra. When xerogel is compared to alcogel (Figs. 4 and 2, respectively), however, there is an observable red shift in the Soret bands from 393 to 404 nm for HmP–IX and from 390 to 400 nm for OEP, with a characteristic broadening at higher concentrations of the porphyrins (Fig. 4). This fact is explained by many investigators as due to agglomeration of tetrapyrrole macrocycles [33–35]. A calculation based on the method given for alcogel (see Eq. (1)–(7)) yielded the following parameters characteristic of the dimerization and trimerization of HmP–IX in xerogel: $\varepsilon_{mon} = 3.3 \times 10^5$, $\varepsilon_{dim} = 2.7 \times 10^3$, $\varepsilon_{trim} = 0$, $\log K_{dim} = 6.72$ and $\log K_{trim} = 4.75$. For OEP, the parameters were $\varepsilon_{mon} = 2.4 \times 10^4$, $\varepsilon_{dim} = 1.1 \times 10^3$, $\varepsilon_{trim} = 0$, $\log K_{dim} = 6.99$ and $\log K_{trim} = 3.41$. This calculation is only a very crude approximation, since the determination coefficients R^2 for HmP–IX and OEP in xerogel were 0.95 and 0.91, respectively. Nevertheless, it provides strong support for the conclusion about the predominance of porphyrin dimers over higher forms of aggregation in the xerogel. Still, it cannot be precluded that the red shift in the Soret bands is related to the interaction of porphyrin molecules with silica walls, probably through the formation of hydrogen bonds, as was found earlier [29].

The essential difference between alcogel and xerogel is in the shape of the Q bands. In the case of xerogel, only two components are observed, contrary to alcogel, where four components are present. This fact is directly related to the well-known change in the symmetry of porphyrins from D_{2h} for the dication H_4P^{2+} to D_{4h} for the free-base porphyrin H_2P. From the above, it is quite evident that porphyrins exist in xerogel predominantly as dications. The concentration of free-base forms is very low and, additionally, the Q bands originating from free-base forms overlap with those from dications.

The observed split of the Soret band in the excitation spectra for octaethylporphine and hematoporphyrin IX into two peaks (Fig. 5) suggests the probable formation of H-type (face-to-face) and J-type (face-to-tail) agglomerates of the free-base porphyrins and their dications. This is in agreement with the exciton theory, in which the excited-state energy level of a monomeric dye splits into two during aggregation [35]. The emission spectra (Fig. 6) contain two bands at 612 and 627 nm for HmP–IX and at 603 and 620 nm for OEP. These bands probably correspond to the presence of dications and free-base porphyrins. During the transition from alcogel to xerogel, there can be observed a blue shift in the bands to 600 and 592 nm and the emergence of a new band near 650 nm,

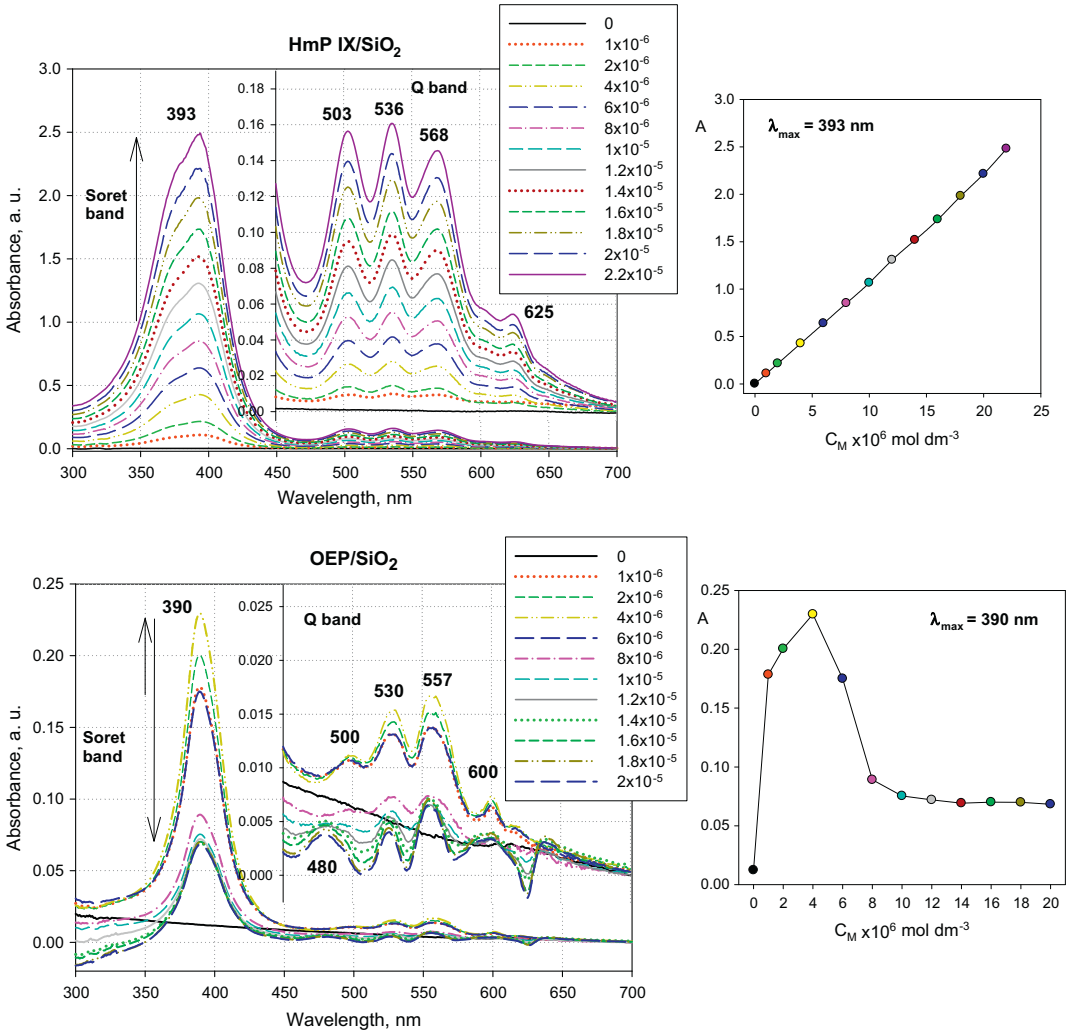

Fig. 2. UV–Vis absorption spectra of HmP–IX and OEP intercalated in SiO_2 alcogel registered 1 week after gelation (the numbers denote the initial concentrations of the porphyrins in silica sol).

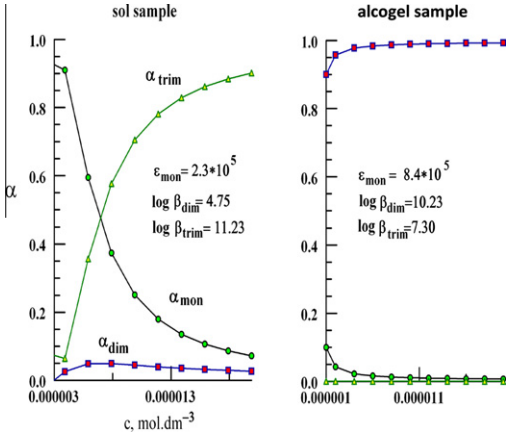

Fig. 3. Comparison of molar fractions (α) of OEP monomers, dimers and trimers in sol and alcogel samples (alcogel 12 weeks after gelation).

which is probably related to the agglomeration of free-base porphyrins and their protonated forms. On the other hand, it is well known that agglomerated and protonated forms of porphyrins have less intense fluorescence compared to free-base porphyrin monomers [36]. Our investigations show, however, that this statement is not true of sol–gel systems, where the dimerized porphyrins are characterized by very strong red fluorescence, more intense than that of porphyrins dissolved in alcogel. This may be due to many factors, such as different dielectric constants of the medium, interaction of the dimerized species with silica walls and/or a difference in the screening of the photoluminescence center by the solvent molecules.

It must be emphasized that outside of optical applications, silica materials should have very small pore sizes; and if functionalized porphyrin systems are used as biocatalysts or chemical sensors, a proper balance between non-leaching of the entrapped bioactive porphyrins and their accessibility to the reagents becomes really important [37]. Textural characterization of the silica xerogel based on N_2 adsorption revealed a microporous character of the adsorbent. The micropore surface area was 411.15 m^2/g, while BET surface area was 537.25 m^2/g. Apart from the micropores, meso- and macropores with diameters of 17–3000 Å were also present in the silica structure. Their participation in the overall pore volumes, however, was minor, namely 0.046 cm^3/g per 0.252 cm^3/g of the total pore volume; nevertheless, it is evident that the accommodation of J- and H-dimers of porphyrins inside the gel structure is possible without steric obstacles.

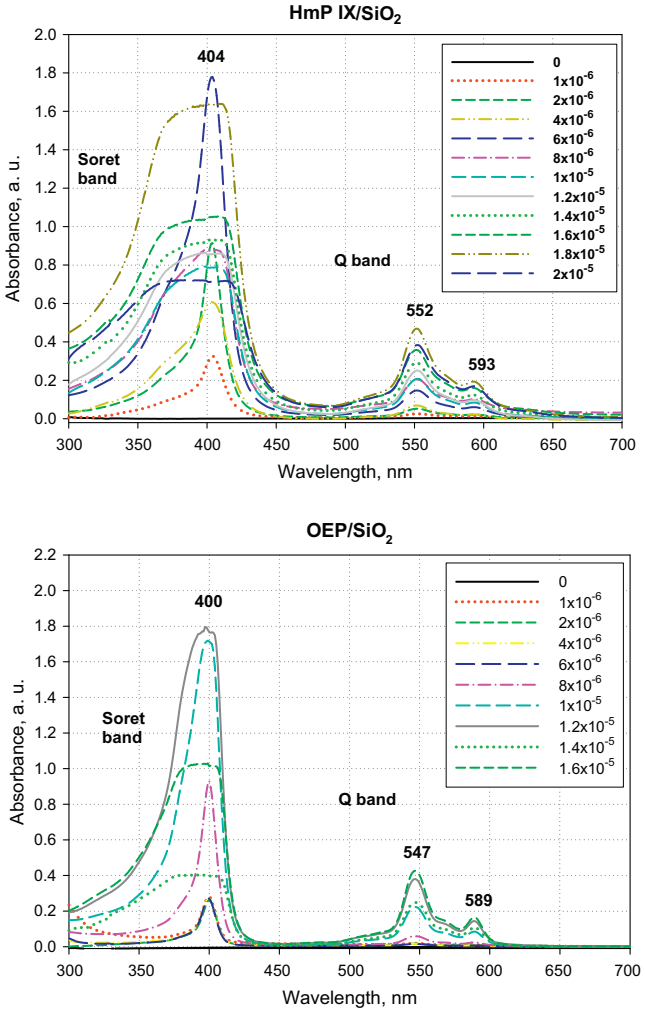

Fig. 4. UV–Vis absorption spectra of HmP–IX and OEP intercalated in SiO_2 xerogel (7 months after gelation; the numbers denote the initial concentrations of the porphyrins in silica sol).

3.2. Biotransformation of α-pinene by OEP and HmP–IX encapsulated in silica

The initial investigation was aimed at evaluating the potential of porphyrins encapsulated in silica gel for α-pinene light-promoted biotransformation with oxygen dissolved in the system. Oxidation was carried out over the entire spectral range of visible light because photons with wavelengths up to 700 nm are the most effective for photochemical purposes, while at wavelengths below 300 nm in the direct beam, no solar photons are detectable at the Earth's surface [38]. The photoreaction was carried out at the highest possible concentration of the porphyrins in the materials ($\sim 4 \times 10^{-4}$ M). Drastic differences in bioactivity were observed between OEP/SiO_2 and HmP–IX/SiO_2 in all solvents used (Fig. 7). In chloroform, for example, the yield of products was 6.5-fold higher for the OEP/SiO_2.

The considerable differences in the photobiocatalytic performance of the two intensive luminescent materials studied may result from the strong interaction of the electron-accepting carboxyl groups of HmP–IX with silica, and the much stronger electron donating ability of OEP, which makes the central cavity of the porphyrin ring less electrophilic than in the case of HmP–IX/SiO_2 [39]. According to some investigators, the interaction of porphyrin molecules with silanol groups (Si–OH) through hydrogen bonds promotes non-radiating fluorescence decay of porphyrins, whereas the covalent bond between porphyrin molecules and silica walls in the interior pores of the gel prevents that process [37]. The fact that HmP–IX in silica preserves fluorescence, but significantly loses photoactivity may be attributed to its chemical binding with SiO_2, which probably hinders intersystem crossing from the singlet excited state of the porphyrin to the triplet state, which is a crucial step for photochemical activation of dioxygen.

According to GC–MS data, the main ultimately detectable oxidation products for both porphyrins were pinocarvone, *trans*-pinocarveol and myrtenol, compounds of a high commercial value. The increase in the pinocarveol content in the reaction mixture after addition of the reducing agent PPh_3 additionally pointed to pinocarveyl hydroperoxide as a transitional photooxidation product. The structures of the obtained compounds were consistent with those previously formed in the biotransformation of α-pinene or its enzymatic degradation with some genera of bacteria and fungi [40–42]. Recently, hydroperoxides have been found to be key intermediates in the biotransformation pathway of pinene [43]. Thus, the activity of the examined OEP in a sol–gel matrix can mimic the catalytic oxidative properties of α-pinene monooxygenase and seems to proceed along similar stages as microbial conversions. However, studies on oxidative biotransformation of monoterpenes by most bacterial and fungal monooxygenases [1,44] as well as biomimetic catalysts to metalloenzymes [45] show that *trans*-pinocarveol and pinocarvone are generated as main products in the biotransformation of β-pinene rather than α-pinene. It must be noted that photooxidation of β-pinene by OEP and HmP–IX in a solution system resulted in preferential production of myrtenol, with lower amounts of myrtenal and pinocarvone (data not shown).

Contrary to the observations of some authors studying transformation of monoterpenes by microbial and plant cells [46,47], we found that pinocarvone does not derive from *trans*-pinocarveol. This finding was corroborated by an independent reactivity experiment in which no oxidative products were detected under typical reaction conditions using *trans*-pinocarveol or myrtenol as substrates. Therefore, it can be concluded that all three products: *trans*-pinocarveol, myrtenol and pinocarvone are the result of independent biotransformation reactions of α-pinene at different oxidation rates. Additional support for the above conclusion comes from the fact that the kinetics of the process is of the first order with respect to α-pinene concentration. The straight-line dependence of log (c/co) vs. time t (where co is the initial concentration of pinene) confirms the first-order character of the biotransformation reaction (Fig. 8) with the rate constant $K = 0.013$/h.

3.3. Influence of organic solvent and porphyrin concentration in silica gel on biotransformation yield

Seven organic solvents with various polarities were tested for their ability to enhance α-pinene photoconversion by HmP–IX and OEP entrapped in silica gel. Only in the case of methanol and acetonitrile was slow sedimentation of silica particles observed. A variation in the distribution of oxygenated products in the different media was noted (Fig. 7). The reason for the distinctly different molar ratios of, for instance, myrtenol/pinocarvone, especially in chloroform, dichloromethane, acetone and acetonitrile is rather complex. It can be explained by solvent effects on the rate of the consecutive reaction steps and/or the rate of decay of reactive oxygen species. We believe that it is especially the different dielectric constants and, hence, the different polarities of the solvents that determine the lifetime and rates of formation of active intermediates such as free radicals and singlet oxygen as well as subsequent recombination of these species. Taking into account the fact that a photocatalytic reaction may involve electron abstraction from pinene either by an excited photocatalyst or by

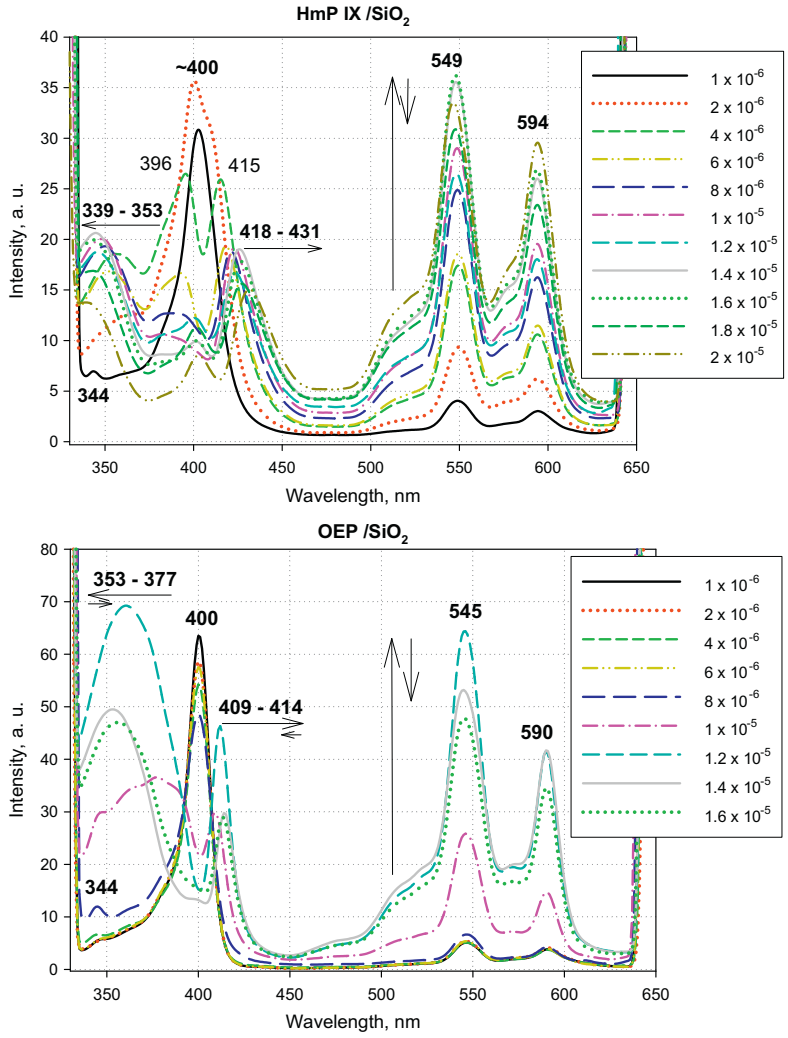

Fig. 5. Excitation spectra of the porphyrins in xerogel (16 months after gelation, emission at 650 nm).

singlet oxygen, we cannot exclude the influence of the solvent on the easy transfer of the electron in the system. Similar solvent effects have already been described in the literature [48]. The present results clearly indicate that myrtenol and part of pinocarveol are formed in a pathway that involves different reactive intermediate species than those involved in the hydroperoxide pathway of pinocarvone formation.

Maximum yields of all photooxidation products were obtained in non-polar solvents, e.g., chloroform and methyl chloride. Hydrophilic solvents such as, for example, EtOH were substantially less efficient in terms of their ability to maintain active porphyrins in sol–gel, probably because alcohols quench active oxygen species or pinene radical cations. In an investigation of the photooxygenation of styrene, no active oxygen species have been detected in alcohol reaction systems [49]. The highest bioconversion of α-pinene by OEP/SiO_2 and HmP–IX/SiO_2 was obtained in chloroform, probably as a result of the fact that singlet oxygen as the primary oxygen agent responsible for the photooxidation by light-sensitive catalysts [50] has a relatively long lifetime in this solvent [51].

Light-promoted addition of singlet oxygen to pinene is known to produce hydroperoxides that originate from an ene-type reaction [52,53]. Therefore, the product profile of the OEP/SiO_2 system was also analyzed after reducing the expected hydroperoxides to corresponding alcohols. When PPh_3 was added to the reaction mixture, pinocarvone almost completely disappeared in favor of *trans*-pinocarveol. This means that pinocarvone derived from a pinocarveyl hydroperoxide intermediate and needs to be interpreted as a secondary product of photocatalysis. It probably arose from the decomposition of the hydroperoxide during thermolysis in the GC injector port; photochemical transformation of the hydroperoxide (on long exposure of the photocatalyst to irradiation) can be neglected as a source of pinocarvone. Myrtenol, another product of photocatalysis, is not an ene product typical of the α-pinene reaction with $^1O_2$, and thus, it might have arisen from a radical-type background reaction. It is interesting to note that hydroperoxides, as unstable compounds, have been reported to be decomposed under photocatalytic conditions with a broad variety of side products formed or in a GC system with alcohol and pinene oxide as the only products [54,55]. The behavior of the studied photocatalyst toward α-pinene can be compared neither to that of some groups of manganese porphyrin catalysts which use peroxides as oxidants nor to porphyrin photocatalysts which afford the formation of mixtures of pinene oxide, verbenol, verbenone and myrtenol [7,8,53]. However, our system shows a certain resemblance to the porphyrin-based photosensitized reaction leading to the formation of pinocarveol and myrtenol as main products, preceded by reduction of the corresponding hydroperoxides [14]. As far as we know, pinocarvone from α-pinene has only been obtained in UV-catalyzed oxidation involving the use of

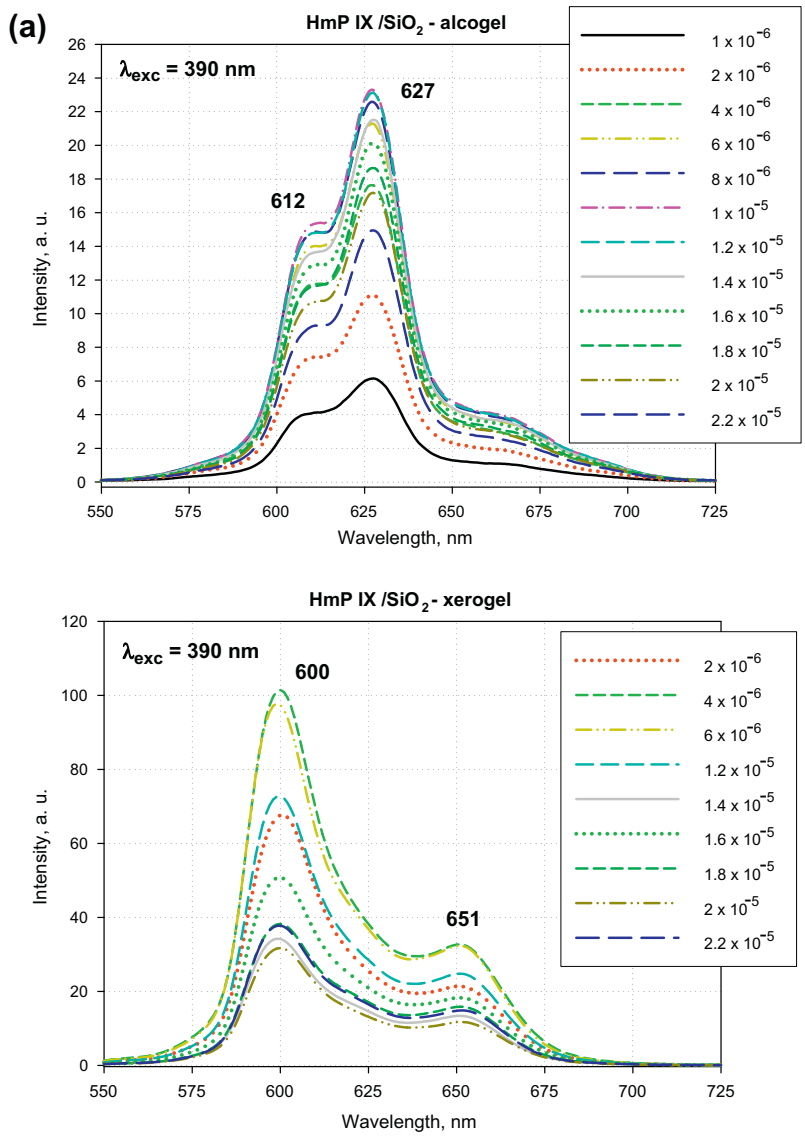

Fig. 6. Comparison of the emission spectra of HmP–IX (a) and OEP (b) in alco- and xerogel (excitation wavelength 390 nm).

H_2TPP as photosensitizer and some very toxic chemicals: acetic anhydride, pyridine, (dimethylamino)pyridine and base [56]. The literature points out that allylic oxidation of α-pinene also gives rise to verbenyl hydroperoxide (and myrtenyl hydroperoxide) derivatives and subsequently to the formation of verbenol and verbenone [57,58].

A free-radical chain mechanism is also suggested in photooxidation reactions. A broad product mixture of allylic and epoxide oxidation products usually arises from typical radical-initiated autoxidation [20,53]. Since we obtained alcohol and hydroperoxide (and ketone from it) only, with no verbenyl-derived products and neither epoxide nor corresponding glycol derivatives, we suggest that phototransformation of α-pinene by porphyrins in silica gel involves a cooperative mechanism of photooxidation based on two possible routes. The first pathway, consisting in electron abstraction from substrate by the light-excited OEP/SiO_2 matrix, can lead to the formation of minor components during a radical autoxidation mechanism, while the most abundant compounds, pinocarveyl hydroperoxide is formed through a photosensitized reaction with singlet oxygen (either by electron transfer from α-pinene to $^1O_2$ or via a radical mechanism). These two alternative pathways (type I and II) are well documented in the literature [11,50]. As has been postulated previously, the mechanism of photooxidation is determined by the concurrent involvement of the reactive oxygen species: singlet oxygen ($^1O_2$), superoxide radical anions ($O^{2\cdot-}$) and hydroxyl radicals [59,60].

Trans-pinocarveol and myrtenol are formed, presumably, via rapid decomposition of the hydroperoxide radical in the radical chain mechanism, as has been reported by Schrader et al. [61]. McMorn et al. [57] also suggest that oxidation of α-pinene to verbenone using a silica–titania co-gel catalyst proceeds probably via the formation of a hydroperoxy intermediate. No attempt has been made to optimize this result, but it is apparent that OEP in silica gel could provide a novel biomimetic pathway to pinocarvone.

In a subsequent experiment, the porphyrins at various concentrations in the sol–gel matrix (ranging from 1×10^{-6} to 2.2×10^{-5} M) for the photooxidation of α-pinene were examined to investigate product yields and catalytic activity and also to examine the correlation between the biocatalytic efficiency of the porphyrins in SiO_2 and their intensity of fluorescent emission and absorbance. In this experiment, we also wanted to determine the effect of porphyrin aggregation on the yield of the photooxidation reaction. The results were studied considering the efficiency of the photocatalysts in terms of turnover number (*TON*), defined as the

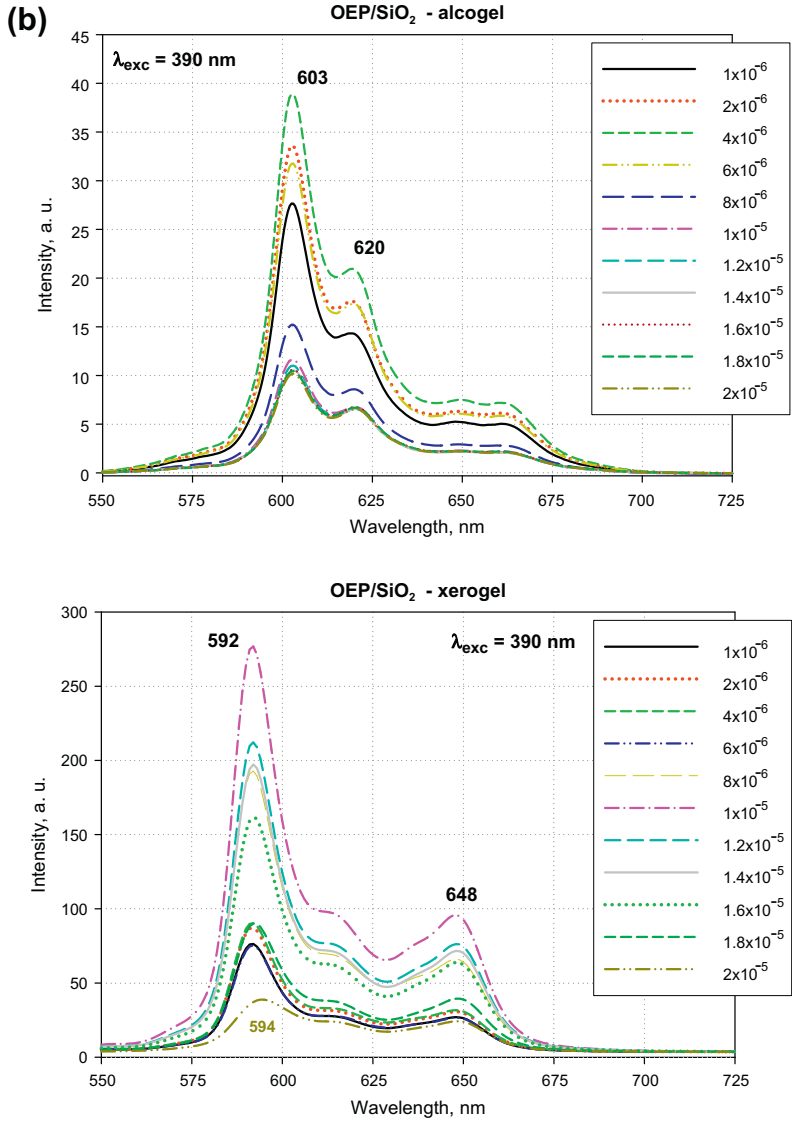

Fig. 6 (*continued*)

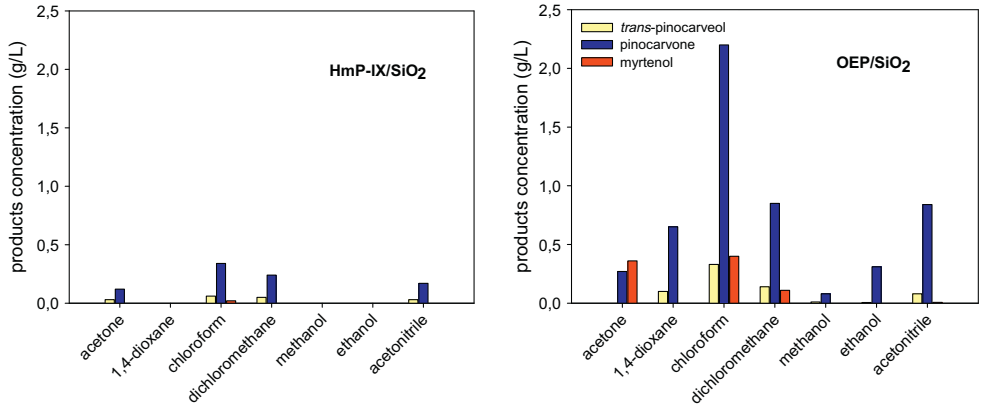

Fig. 7. Comparison of biomimetic activity of HmP–IX and OEP encapsulated in silica gel in the process of α-pinene photooxidation in different organic solvents.

number of moles of product formed per mole of porphyrin per hour. The biocatalytic efficiency of the porphyrins entrapped in the sol–gel matrix was found to be positively correlated with their intensity of fluorescent emission and absorbance over the range of their concentrations studied in sol. The maximum *TON* was reached at 6×10^{-6} M for OEP (Fig. 9). Close to this OEP concentration, the highest luminescence intensity and sharpness of the relative Soret band was observed in alcogel, which rules out the

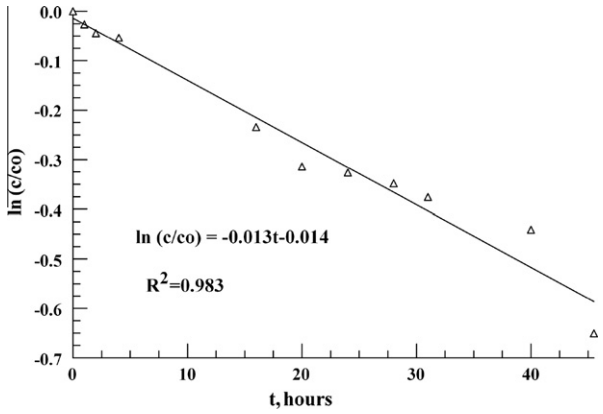

Fig. 8. The progress of α-pinene biotransformation according to first-order kinetics (*c* – concentration of α-pinene at time *t*, *co* – initial concentration of pinene).

formation of higher aggregated species of the porphyrin. At high concentrations of the porphyrin in silica, a drop in the catalytic effectiveness occurred. This is in agreement with the more general rule that the formation of a dication and higher-order aggregates decreases the photoactivity of photosensitizers [62–64], as the presence of porphyrin stacking does not allow optimal interaction of α-pinene with macrocycles [65]. However, contrary to expectation, octaethylporphine in xerogel showed maximum absorbance and enhanced luminescence in the concentration region between 1×10^{-5} and 1.4×10^{-5} M. In all probability, this was caused by the formation of associate porphyrin structures, which, by transferring energy from one to another led to a radiative transition from the OEP/SiO_2 excited state to its singlet ground state, concurrently with photochemical activation of dioxygen. In turn, HmP–IX/SiO_2 showed residual activity over the entire range of concentrations studied, with slightly higher values at 2.2×10^{-5} M (data not shown). This indicates that the poor catalytic behavior of hematoporphyrin in silica gel has no relation to its agglomeration.

3.4. Comparison of homogeneous and heterogeneous systems

In all our earlier studies regarding the photooxidation of limonene, both the OEP and the HmP–IX porphyrin were very active in a homogeneous system. Whenever photosensitizers are immobilized, their photophysical properties as well as photodegradation and aggregation tendencies change, and these changes may have an effect on the profile and yields of photooxidation products of a substrate [66]. We compared the photooxidation of α-pinene in a homogenous and a heterogeneous system using the same total amount of catalyst. In the case of OEP, the overall characteristics of the reaction were similar (Fig. 10). In comparison with OEP, HmP–IX in the homogeneous system showed lower yields of products due to its low solubility in chloroform used as solvent in the photoreaction. As expected from the previous results with heterogeneous systems, HmP–IX lost its photocatalytic activity when intercalated in SiO_2.

The correlation between the photoactivity of free-base OEP in organic solutions and that entrapped in silica matrices indicates that the strategy of its incorporation into the transparent matrix was successful, as the photoactivity of OEP in the heterogeneous system was exactly the same as in the homogeneous system. The photoactivity was preserved despite the fact that the structure of the silica matrix, with some of its pores being closed, might hinder the access of oxygen and α-pinene to the catalytic site and diffusion of the oxidation products into the reaction medium. This result also stands in contradiction to the general rule that immobilized photosensitizers show reduced quantum yield of $^1O_2$ generation [50]. This is additional evidence both for the efficiency of the new porphyrin photocatalyst in SiO_2 matrix and for the existence of a non-$^1O_2$ pathway for the biotransformation of α-pinene.

As mentioned before, OEP at concentrations up to 6×10^{-6} M exists in xerogel mainly in the form of dimers rather than higher-order aggregated porphyrin species, as confirmed by the splitting of the excitation band (see Fig. 5). As a consequence, the OEP-doped xerogel employed in the experiment showed a sharp Soret band. From most of the above data, it is possible to rationalize the pathways for the biomimetic oxidation of terpenes by the porphyrin encapsulated in silica gel. We propose that photooxidation of monoterpenes involves the participation of two species, dimers and dications of OEP in SiO_2. As a conclusion, we propose a hypothetical primary step of the mechanism of α-pinene photooxidation by OEP/SiO_2 (Scheme 1). The essential, photoinduced process would involve transfer of protons from the dimeric form of the porphyrin dication to the lone electron pairs of siloxane oxygen (in ≡Si—O—Si≡) or passing of protons to unbound silanol groups of the silica network. The resulting excited porphyrin in the triplet state could then react in one of two ways, via type I or II photooxygenation mechanism. In the case of HmP–IX, the silanol groups and the lone electron pairs inside the silica

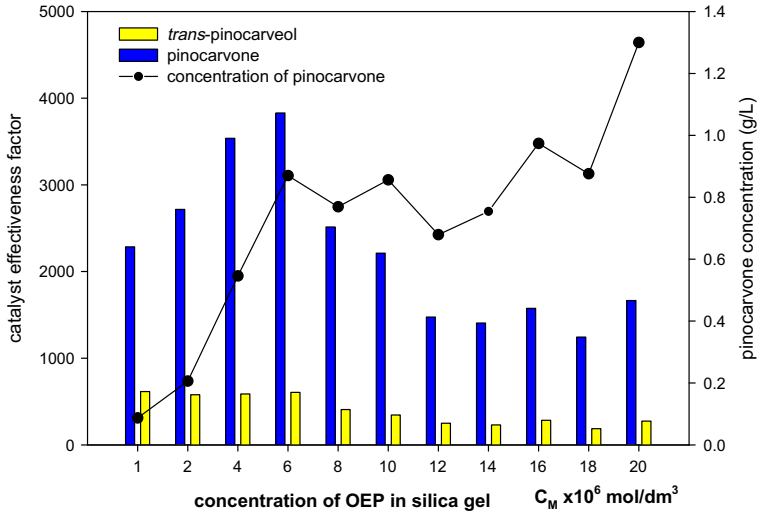

Fig. 9. Effect of the initial concentration of OEP in silica gel on its biocatalytic efficiency in α-pinene photooxidation.

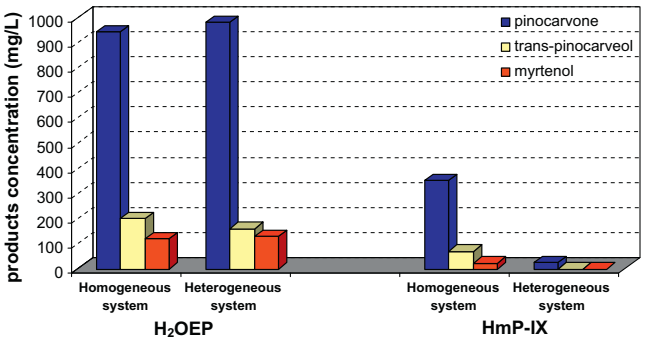

Fig. 10. Comparison of product yields from the photooxidation of α-pinene in a homogeneous system vs. a heterogeneous system based on the silica-immobilized porphyrins, HmP–IX and OEP.

pores are blocked by the electrophilic group of HmP–IX, making transfer of protons from the excited porphyrinic complex impossible.

During the course of photooxidation, the reaction solution remains colorless. The stability and reusability of OEP/SiO_2 in photocatalytic oxidation of pinene studied within four catalytic cycles is shown in Fig. 11. The OEP/SiO_2 catalyst could be repeatedly used for 4 successive biotransformations of each 20-h cycle with the total turnover number of up to 12,000. The most significant loss of photocatalytic activity (about 30%) was observed after the first cycle. Then, the activity was maintained at the same level for another 2 cycles to fall by 20% after the fourth cycle. The porphyrin immobilized inside the matrix retained 50% of its initial activity. As was shown in UV–Vis reflectance spectra (Fig. 11), the decrease in the absorption intensity after the first cycle could point to leaching of the catalyst from the silica support into the solution. However, the experiments with filtrates recovered after removal of the catalyst demonstrated residual activity for α-pinene photoconversion in the filtrate, but only in that obtained after the first re-use of the catalyst. This can be explained by the photobleaching of the catalyst and its consequent release into solution in an inactive form, which is not detectable by visible spectroscopy. It has to be emphasized that the OEP/SiO_2 catalyst practically did not change its visible spectrum over the four cycles performed, in contrast to free OEP in the homogeneous system, which exhibited changes in the UV–Vis spectra (possibly by protonation) and lost its activity (data not shown). The OEP/SiO_2 is easily removable by filtration

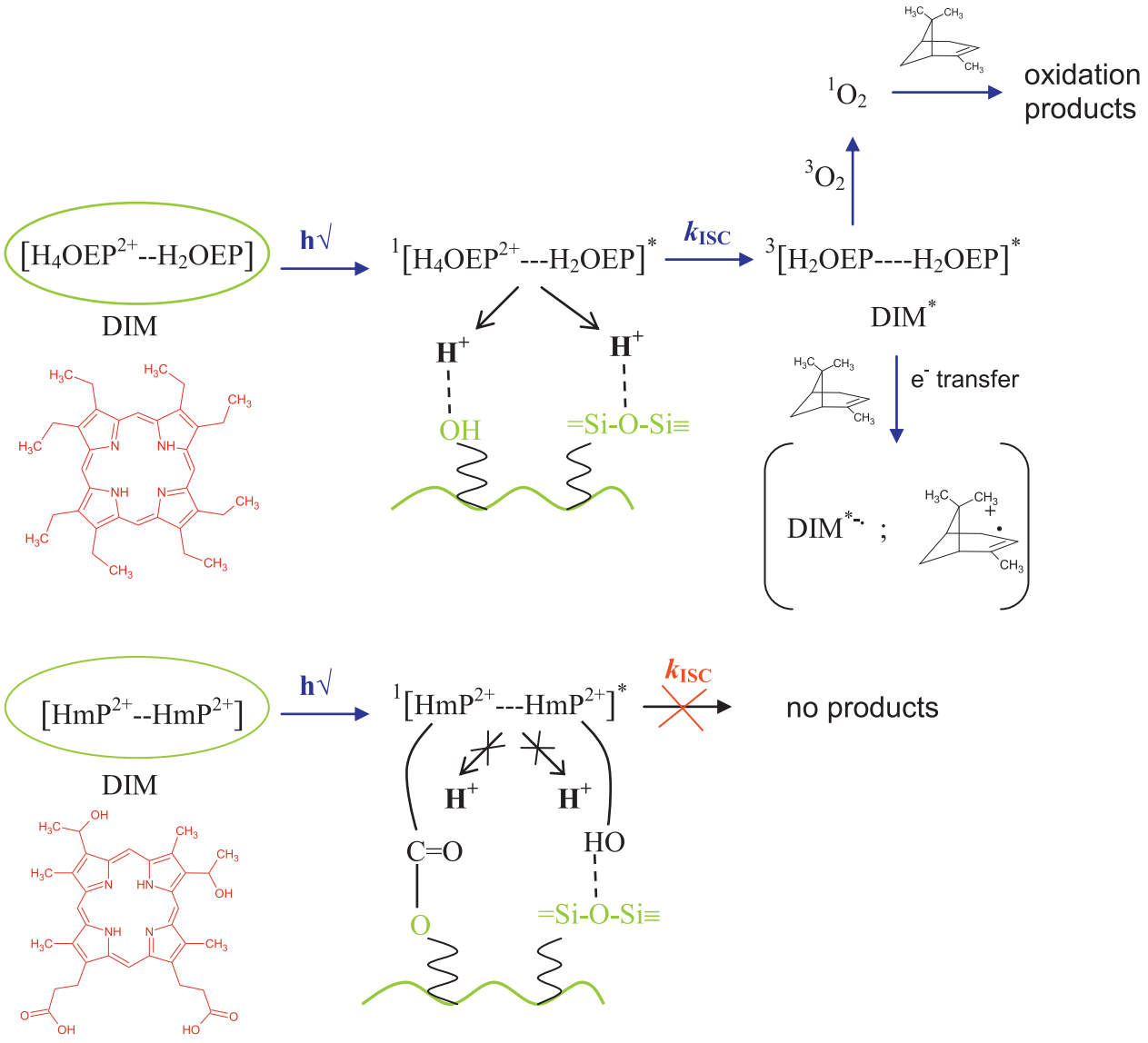

Scheme 1.

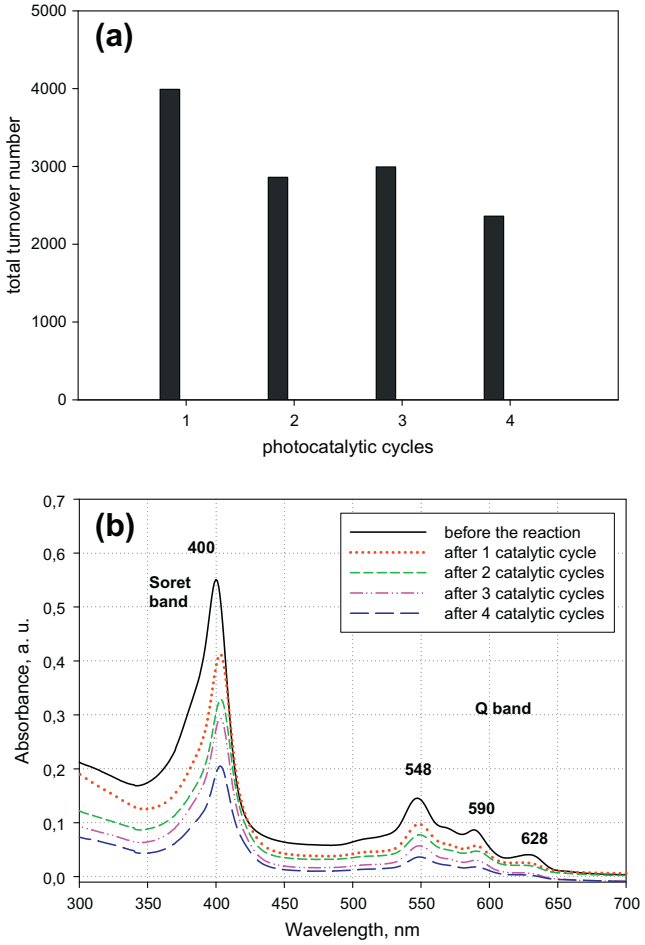

Fig. 11. Reusability of OEP/SiO_2 in the photocatalytic oxidation of pinene (a) and UV–Vis reflectance spectra showing its stability (b); (concentration of OEP in silica gel: 6×10^{-6} M).

from the reaction mixture, greatly simplifying the isolation of the products. Moreover, OEP/SiO_2 is recyclable and has been reused up to three times without any appreciable loss of catalytic activity. This stability is not only due to the physical entrapment but also to the multiple additional interactions with SiO_2 through hydrogen bonds, ionic or hydrophobic forces. Although the reported results are promising, additional research is needed to develop a method for decreasing porphyrin photobleaching for use in the biotransformation of terpenes.

In our study, we obtained pinocarvone that can be found, though unfortunately only in small amounts, for example, in extracts of *Hyssopus officinalis* and *Chrysanthemum parthenium* as well as in Chamomile and Eucalyptus essential oils. Pinocarvone has practical applications as a flavor compound, a cockroach attractant [67] and a key intermediate for the manufacture of various fine chemicals including tricyclic lactones widely used as perfume and flavor ingredients [68].

4. Conclusions

1. Encapsulation of octaethylporphine in silica gel generates biomaterials with a high fluorescence intensity and photocatalytic activity, which resemble enzymes involved in monoterpene biotransformation. By contrast, hematoporphyrin encapsulated in silica gel preserves its luminescence properties only.
2. It is suggested that the lack of photocatalytic activity in hematoporphyrin is caused by its covalent binding with the silica network, which probably impedes the formation of active oxygen species.
3. The decrease in the photocatalytic efficiency with the rise in octaethylporphine concentration accompanies the formation of higher-than-dimer aggregates of this porphyrin in silica.
4. α-Pinene oxidation probably occurs with the participation of singlet oxygen or/and oxygen radicals, generated by partially protonated porphyrin dimers.
5. The final oxidation products, namely *trans*-pinocarveol, pinocarvone and myrtenol, are formed independently in the first-order reaction of α-pinene oxidation.
6. The octaethylporphine photocatalyst in silica gel, as compared to its free-base form in the homogeneous system, is easily and efficiently recycled within four catalytic cycles with the total photooxygenation turnover number of up to 12,000.

References

[1] J.L. Bicas, A.P. Dionísio, G.M. Pastore, Chem. Rev. 109 (2009) 4518.
[2] W. Duetz, H. Bouwmeester, J.B. van Beilen, B. Witholt, Appl. Microbiol. Biotechnol. 61 (2003) 265.
[3] K.S. Suslick, in: K. Kadish, K. Smith, R. Guillard (Eds.), The Porphyrin Handbook, Academic Press, New York, 1999, p. 41.
[4] J. Groves, J. Porphyr. Phthalocya. 4 (2000) 350.
[5] J. Bernadou, B. Meunier, Adv. Synth. Catal. 346 (2004) 171.
[6] L. Que, W. Tolman, Nature 455 (2008) 333.
[7] V. Maraval, J. Ancel, B. Meunier, J. Catal. 206 (2002) 349.
[8] C.-C. Guo, W.-J. Yang, Y.-L. Mao, J. Mol. Catal. A: Chem. 226 (2005) 279.
[9] E.R. Milaeva, O.A. Gerasimova, A.L. Maximov, E.A. Ivanova, E.A. Karachanov, N. Hadjiliadis, M. Louloudi, Catal. Commun. 8 (2007) 2069.
[10] J.J. Inbaraj, M.V. Vinodu, R. Gandhidsan, R. Murugesan, M. Padmanabhan, J. Appl. Polym. Sci. 89 (2003) 3925.
[11] A. Griesbeck, T. El-Idreesy, A. Bartoschek, Adv. Synth. Catal. 346 (2004) 245.
[12] A. Griesbeck, T. El-Idreesy, Photochem. Photobiol. Sci. 4 (2005) 205.
[13] C.J. Rogers, T.J. Dickerson, P. Wentworth Jr, K.D. Janda, Tetrahedron 61 (2005) 12140.
[14] S.M. Ribeiro, A.C. Serra, A.M.d'A.R. Gonsalves, J. Catal. 256 (2008) 331.
[15] F. Bedioui, Coord. Chem. Rev. 144 (1995) 39.
[16] S. Evans, J.R. Lindsay Smith, J. Chem. Soc. Perkin Trans. 2 (2001) 174.
[17] G. Huang, C.-C. Guo, S.-S. Tang, J. Mol. Catal. A: Chem. 261 (2007) 125.
[18] S. Campestrini, B. Meunier, Inorg. Chem. 31 (1992) 1999.
[19] R. Gerdes, O. Bartels, G. Schneider, D. Wöhrle, G. Schulz-Ekloff, Polym. Adv. Technol. 12 (2001) 152.
[20] S. Nakagaki, F. Benedito, F. Wypych, J. Mol. Catal. A: Chem. 217 (2004) 121.
[21] F.C. Skrobot, A.A. Valente, G. Neves, I. Rosa, J. Rocha, J.A.S. Cavaleiro, J. Mol. Catal. A: Chem. 201 (2003) 211.
[22] J. Haber, K. Pamin, J. Połtowicz, J. Mol. Catal. A: Chem. 224 (2004) 153.
[23] V.B. Kandimalla, V.S. Tripathi, H. Ju, Crit. Rev. Anal. Chem. 36 (2006) 3.
[24] J.C. Biazzotto, E.A. Vidoto, O.R. Nascimento, Y. Iamamoto, O.A. Serra, J. Non-Cryst. Solids 304 (2002) 101.
[25] M.S.M. Moreira, P.R. Martins, R.B. Curi, O.R. Nascimento, Y. Iamamoto, J. Mol. Catal. A: Chem. 233 (2005) 73.
[26] A.T. Papacídero, L.A. Rocha, B.L. Caetano, E. Molina, H.C. Sacco, E.J. Nassar, Y. Martinelli, C. Mello, S. Nakagaki, K.J. Ciuffi, Colloids Surf. A 275 (2006) 27.
[27] J.-H. Cai, J.-W. Huang, P. Zhao, Y.-J. Ye, H.-C. Yu, L.-N. Ji, J. Photochem. Photobiol. A 2–3 (2009) 236.
[28] W. Kim, J. Park, H.J. Jo, H.-J. Kim, W. Choi, J. Phys. Chem. C 112 (2008) 491.
[29] M. Trytek, J. Fiedurek, A. Lipke, S. Radzki, J. Sol–Gel Sci. Technol. 51 (2009) 272.
[30] S. Brunauer, P.H. Emmett, E. Teller, J. Am. Chem. Soc. 60 (1938) 309.
[31] L. Weber, R. Hommel, J. Behling, G. Haufe, H. Hennig, J. Am. Chem. Soc. 116 (1994) 2400.
[32] S. Takagi, D. Tryk, H. Inoue, J. Phys. Chem. B 106 (2002) 5455.
[33] S.B. Brown, M. Shillcock, Biochem. J. 153 (1976) 279.
[34] M.-S. Choi, Tetrahedron Lett. 49 (2008) 7050.
[35] E. Fagadar-Cosma, C. Enache, R. Tudose, I. Armenau, E. Mosoarca, D. Vlascici, O. Costisor, Rev. Chim. (Bucuresti) 58 (2007) 451.
[36] V.S. Chirvony, A. Van Hoek, V.A. Galievsky, I.V. Sazanovich, T.J. Schaafsma, D. Holten, J. Phys. Chem. 104 (2000) 9809.
[37] M.A. García-Sánchez, V. De la Luz, M.L. Estrada-Rico, M.M. Murillo-Martínez, M.I. Coahuila-Hernández, R. Sosa-Fonseca, S.R. Tello-Solís, F. Rojas, A. Campero, J. Non-Cryst. Solids 355 (2009) 120.
[38] B. Pohlmann, H.D. Scharf, U. Jarolimek, P. Mauermann, Sol. Energy 61 (1997) 159.
[39] K.M. Kane, C.R. Lorenz, D.M. Heilman, F.R. Lemke, Inorg. Chem. 37 (1998) 669.
[40] D. Busmann, R.G. Berger, in: H. Maarse, D.G. Van Der Heij (Eds.), Trends in Flavour Research, Elsevier, Amsterdam, 1994.
[41] N. Savithiry, D. Gage, W. Fu, P. Oriel, Biodegradation 9 (1998) 337.
[42] H. Schewe, B.-A. Kaup, J. Schrader, Appl. Microbiol. Biotechnol. 78 (2008) 55.
[43] U. Krings, N. Lehnert, M. Fraatz, B. Hardebusch, H. Zorn, R. Berger, J. Agric. Food Chem. 57 (2009) 9944.

[44] M. Lindmark-Henriksson, Biotransformations of Turpentine Constituents. Oxygenation and Esterification, PhD thesis, Mid Sweden University, 2003.
[45] M. Caovilla, A. Caovilla, S.B.C. Pergher, M.C. Esmelindro, C. Fernandes, C. Dariva, K. Bernardo-Gusmão, E.G. Oestreicher, O.A.C. Antunes, Catal. Today 133–135 (2008) 695.
[46] Y. Noma, T. Hashimoto, S. Uehara, Y. Asakawa, Flavour Fragrance J. 25 (2010) 161.
[47] M. Lindmark-Henriksson, D. Isaksson, T. Vaněk, I. Valterová, H.-E. Högberg, K. Sjödin, J. Biotechnol. 107 (2004) 173.
[48] M.D. Hughes, Y.-J. Xu, P. Jenkins, P. McMorn, P. Landon, D.I. Enache, A.F. Carley, G.A. Attard, G.J. Hutchings, F. King, E.H. Stitt, P. Johnston, K. Griffin, C.J. Kiely, Nature 437 (2005) 1132.
[49] Y. Ren, Y. Che, W. Ma, X. Zhang, T. Shen, J. Zhao, New J. Chem. 28 (2004) 1464.
[50] M. DeRosa, R. Crutchley, Coord. Chem. Rev. 233–234 (2002) 351.
[51] J. Hurst, J. McDonald, G. Schuster, J. Am. Chem. Soc. 104 (1982) 2065.
[52] R. Kenney, G. Fisher, Ind. Eng. Chem. Prod. Res. Dev. 12 (1973) 317.
[53] H. Hennig, D. Rehorek, R. Stich, L. Weber, Pure Appl. Chem. 62 (1990) 1489.
[54] J.E. Ancel, N.V. Maksimchuk, I.L. Simakova, V.A. Semikolenov, Appl. Catal. A: Gen. 272 (2004) 109.
[55] N.I. Kuznetsova, L.I. Kuznetsova, N.V. Kirillova, L.G. Detusheva, V.A. Likholobov, M.I. Khramov, J.-E. Ansel, Kinet. Catal. 46 (2005) 204.
[56] E.D. Mihelich, D.J. Eickhoff, J. Org. Chem. 48 (1983) 4135.
[57] P. McMorn, G. Roberts, G.J. Hutchings, Catal. Lett. 67 (2000) 203.
[58] S.G. Casuscelli, G.A. Eimer, A. Canepa, A.C. Heredia, C.E. Poncio, M.E. Crivello, C.F. Perez, A.A.E.R. Herrero, Catal. Today 133–135 (2008) 678.
[59] J. Chacon, J. McLearie, R. Sinclair, Photochem. Photobiol. 47 (1988) 647.
[60] I. Ahmad, Q. Fasihullah, A. Noor, I. Ansari, Q. Ali, Int. J. Pharm. 280 (2004) 199.
[61] W. Schrader, J. Geiger, D. Klockow, E.H. Korte, Environ. Sci. Technol. 35 (2001) 2717.
[62] R. Gerdes, D. Wöhrle, W. Spiller, G. Schneider, G. Schnurpfei, G. Schulz-Ekloff, J. Photochem. Photobiol. A 111 (1997) 65.
[63] V. Iliev, L. Prahov, L. Bilyarska, H. Fischer, G. Schulz-Ekloff, D. Wöhrle, L. Petrov, J. Mol. Catal. A: Chem. 151 (2000) 161.
[64] C. Tanielian, C. Schweitzer, R. Mechin, C. Wolff, Free Radical Biol. Med. 30 (2001) 208.
[65] R. Paolesse, D. Monti, L. La Monica, M. Venanzi, A. Froiio, S. Nardis, C. Di Natale, E. Martinelli, A. D'Amico, Chem-Eur J. 8 (2002) 2476.
[66] C. Karapire, M. Kus, G. Turkmen, C.C. Trevithick-Sutton, C.S. Foote, S. Icli, Sol. Energy 78 (2005) 5.
[67] C. Nishino, H. Takayanagi, JP Patent 56-30905 A, 1981 (to Mitsubishi Chem. Ind.).
[68] J.J. Becker, US Patent 4273714, 1981 (to Firmenich, S.A.).